^{3}He in Planetary Nebulae: a Challenge to Stellar Evolution Models

Daniele Galli[1], Letizia Stanghellini[2], Monica Tosi[2] and Francesco Palla[1]

ABSTRACT

The discrepancy between the observed abundances of ^{3}He in the interstellar medium and those predicted by stellar and galactic chemical evolution remains largely unexplained. In this paper, we attempt to shed some light on this unsolved problem by presenting a quantitative comparison of the ^{3}He abundances recently measured in six planetary nebulae (IC 289, NGC 3242, NGC 6543, NGC 6720, NGC 7009, NGC 7662) with the corresponding predictions of stellar evolution theory. The determination of the mass of the planetary nebulae progenitors allows us to dismiss, to a good degree of confidence, the hypothesis that the abundance of ^{3}He in the envelope of all low–mass stars ($M \lesssim 2.5\ M_\odot$) is strongly reduced with respect to the standard theoretical values by some mixing mechanism acting in the latest phases of stellar evolution. The abundance versus mass correlation, allowance made for the limitation of the sample, is in fact found to be fully consistent with the classical prediction of stellar evolution. We examine the implications of this result on the galactic evolution of ^{3}He with the help of a series of models with standard and non–standard (i.e. ^{3}He depleted) nucleosynthesis prescriptions in varying percentages of low–mass stars. The results are found to be consistent with the abundances determined in the pre–solar material and in the local interstellar medium *only* if the vast majority of low–mass stars (more than 70–80 %) follows non–standard prescriptions. This implies that either the sample of planetary nebulae under exam is highly biased and therefore not representative of the whole population of low–mass stars, or the solution to the ^{3}He problem lies elsewhere.

Subject headings: galaxies: evolution - nucleosynthesis, abundances; planetary nebulae: individual, central stars, abundances

1. Introduction

Can the observed abundances of ^{3}He be used to set bounds on the standard Big Bang nucleosynthesis models (SBBN)? The issue has been a hot topic for many years, but the answer is still under debate. If the ^{3}He abundance increases with time in the Galaxy, then the lowest observed abundance of this isotope places a *lower* limit to the baryon–to–photon ratio η (see e.g. Yang et al. 1984). Steigman & Tosi (1992), Vangioni-Flam, Olive & Prantzos (1994), and other authors have shown that, neglecting the stellar production of ^{3}He, the models of galactic chemical evolution of light isotopes can be safely used to infer the primordial abundances, and hence to test the SBBN predictions. On the other hand, starting from the classical papers by Iben (1967) and Truran & Cameron (1971), stellar models have always predicted that low–mass stars are strong producers of ^{3}He. When stellar production is included in models for the chemical evolution of the Galaxy, no agreement between observed and predicted ^{3}He abundances can be found (Rood, Steigman & Tinsley 1976; and, more recently, Galli et al. 1995, Olive et al. 1995, Dearborn, Steigman & Tosi 1996, hereafter DST, Fields 1996, Prantzos 1996). Thus, the usefulness of the helium isotope as a “cosmological baryometer” remains highly questionable.

The strongest piece of evidence in favor of ^{3}He production in stars comes from the observation of this isotope in galactic planetary nebulae (PNs). The first detection of ^{3}He in a PN (NCG 3242, by Rood, Bania, & Wilson 1992) confirmed the theoretical prediction that low–mass stars are net producers of ^{3}He. The derived abundance (^{3}He/H $\sim 10^{-3}$) was found to be in good quantitative agreement with the predicted values for stars of about one solar mass. Subsequently, the ^{3}He has been searched for in other PNs, and detected in two other nebulae whose abundances are similar to that of NGC 3242 (see Rood et al. 1995, hereafter RBWB, for an updated review).

[1]Osservatorio Astrofisico di Arcetri, Largo E. Fermi 5, I–50125 Firenze, Italy

[2]Osservatorio Astronomico di Bologna, via Zamboni 33, I–40126 Bologna, Italy

The abundance of ^{3}He in PNs is much higher than that measured in the solar system and in the interstellar medium (ISM) by one to two orders of magnitude. This evidence is the heart of the so-called "^{3}He-problem". Indeed, observations toward a sample of galactic H II regions (Balser et al. 1994) and the very recent measurements by the Ulysses spacecraft in the local interstellar cloud (Gloeckler & Geiss 1996) indicate a value of ^{3}He/H $\sim 10^{-5}$. It appears that the ISM, today as well as at the time of the formation of the Sun, has not been contaminated by the high fractional abundances of ^{3}He observed in the PNs studied by RBWB. Since chemical abundances in PNs are expected to represent the yields of low–mass stars, the question is whether the RBWB sample consists of an exception rather than a rule in the evolution of low–mass stars.

In view of the importance of this argument, we have critically analyzed the problem in the sense of determining reliably the masses of the PN progenitors in the RBWB sample, to check the observed ^{3}He abundance to mass correlation against the stellar models. The basic knowledge of low–mass stellar evolution and of plasma diagnostics allow us to tackle this basic problem in a quantitative way.

The outline of the paper is the following: after a short review of the most recent attempts to solve the ^{3}He problem at a stellar level (Section 2), we determine the progenitor masses of the RBWB sample by using up–to–date observed physical parameters of PNs (Section 3). In Section 4 we discuss the main steps for the calculations of the ^{3}He abundances and we compare the resulting values with the theoretical predictions of stellar models. Finally, in Section 5 we examine the statistical significance of the presently available measurements in PNs in the context of detailed models of galactic chemical evolution.

2. Destruction of ^{3}He in Low–Mass Stars

In an influential paper, Hogan (1995) established a relation between the hypothetical mechanism responsible for the destruction of ^{3}He in stellar envelopes, and the observed anomalies of the carbon isotopic ratio (^{12}C/^{13}C) in a number of evolved stars. In fact, in some stars (field giants, stars in galactic clusters) ^{12}C/^{13}C falls below the predictions of adequate standard models, but only so for masses below $\sim 2\ M_\odot$ (Charbonnel 1994, Fig. 6). These anomalously low ratios can be accounted for by an extra-mixing process occurring after the completion of the first dredge-up, and before the end of the Red Giant Branch (RGB) phase. It is reasonable to think that this process, when present, would drastically alter the post-dredge-up envelope abundance of other fragile isotopes, including ^{3}He.

Following this suggestion, Charbonnel (1994, 1995) found that stellar models of 0.8 and 1 $M_\odot$ with extra-mixing nicely reproduce the low ^{12}C/^{13}C ratios in giant stars, the variation of lithium abundance observed in Pop. II evolved stars, and show a considerable destruction of the envelope ^{3}He abundance. However, this mechanism can operate efficiently only in stars of mass up to $\sim 2\ M_\odot$. The reason is that the occurrence of the mixing process corresponds to the encounter between the advancing hydrogen-burning shell and the discontinuity in chemical composition left beyond by the convective envelope during the dredge-up phase. As mixing cannot penetrate in a region of strong molecular gradient, only after this evolutionary point, and only for those stars where it can actually happen, trace elements in the envelope (e.g. ^{3}He) can be transported down to the hydrogen burning zone and, vice versa, freshly produced elements (e.g. ^{13}C) can be mixed in the convective region up to the stellar surface. For stars more massive than 2 $M_\odot$ the hydrogen-burning shell never reaches the chemically homogeneous region.

Wasserburg, Boothroyd & Sackmann (1995) provided additional support to the extra-mixing hypothesis by computing a set of stellar models for RGB and Asymptotic Giant Branch (AGB) stars undergoing Cool Bottom Processing (CBP), in which an ad hoc mixing mechanism transports stellar fluid elements from the cool bottom of the convective envelope down to some inner layer hot enough for nuclear processing, and vice versa. The model results reproduce the anomalous ^{12}C/^{13}C observed in low–mass RGB stars and, at the same time, show a large destruction of envelope ^{3}He (by a factor ~ 10 in a 1 $M_\odot$ star). The same process can also resolve the puzzling low ^{18}O/^{16}O ratios observed in AGB stars (see also Sackmann & Boothroyd 1996 and Boothroyd & Malaney 1996). Similar results have been obtained by Denissenkov & Weiss (1996) and Weiss, Wagenhuber & Denissenkov (1996), who model deep mixing as a diffusion process and show that a number of observed surface abondance correlations can be quantitatively reproduced, although with slightly different sets of mixing parameters in each case.

In conclusion, non-standard mixing on RGB and/or AGB phases offers an attractive scenario whose basic features can be summarized as follows: (*i*) contrary to the standard view, stars of mass less than 2 $M_\odot$ destroy ^{3}He

during their post-MS evolution and return ^{3}He depleted material to the ISM, consistently with the abundance of ^{3}He measured in the pre-solar material, in galactic H II regions, and in the local ISM; (*ii*) the ^{12}C/^{13}C ratios measured in the envelopes of giants less massive than 2 $M_\odot$, the ^{18}O/^{16}O ratios in the envelopes of AGB stars of the same mass range, and the lithium abundances in metal-poor giants can be quantitatively reproduced; (*iii*) high abundances of ^{3}He are allowed in those PNs whose progenitor mass is larger than 2 $M_\odot$ or did not otherwise undergo extra–mixing. Thus, the ^{3}He puzzle is solved at a *stellar* level.

The question to address now is then: do the PNs with known ^{3}He abundance comply with the scenario outlined above? The answer can only come from an analysis of the mass of their progenitor stars.

3. Planetary Nebulae: the Masses of Progenitor Stars

Central stars (CSs) of PNs are the relics of the AGB stars that have gone through the instability driven ejection of the envelope, after the thermal pulse phase. The progenitor mass is then the stellar remnant mass plus the mass ejected during post–Main Sequence (post–MS) evolution. The direct measure of the ejected mass is not possible, and the study of the CS is not always very straightforward, given that the star is hidden by the surrounding nebula. We determine the progenitor masses through the following observational and interpretative steps:

(*i*) We firstly derive the CS's He II Zanstra temperature, with the method described in Kaler (1983). When assuming that this value is a good approximation of the effective temperature, we make two basic assumptions: the strongest one is that we assimilate the stellar output to a black–body spectrum, the weakest one is to assume that the nebula is thick to the He I–ionizing radiation. In order to calculate Zanstra temperatures we need the values of the Hβ and the He II (λ4686) fluxes, corrected for the atmospheric extinction. Also needed are the angular diameters. We take these basic parameters from the catalog of Cahn, Kaler & Stanghellini (1992, hereafter CKS), which represents the most complete and recent compilation of these PN data. We then use the V and B magnitudes as quoted in Acker et al. (1992, hereafter A92), and, where possible, we use averages of the He II Zanstra temperature derived from the B and V magnitudes, to minimize the errors on the data sets.

(*ii*) To proceed in our analysis, we need an estimate of the distances to the PNs. The first approach is to use statistical distance from CKS. These distances have been derived with the assumption that the ionized mass of PNs is the same for all optically thin PNs, and is a function of the surface brightness for optically thick PNs. These are obviously strong assumptions and result in large distance errors, although the CKS distances are considered among the most reliable statistical distances in the literature, given the very careful calibration (see Terzian 1993). If other (non–statistical) distances are available, we take them into account. The stellar luminosity is then evaluated from the He II temperature and the most reliable distance available.

(*iii*) The derivation of the stellar mass from the observed luminosity and temperature is obtained by placing the star on the $\log L$–$\log T_{\rm eff}$ diagram (see Figure 1), and read off the mass by comparing its position with the synthetic evolutionary tracks (Stanghellini & Renzini 1993). It is worth noting that these tracks have been calculated for H-burning CS, while there are indications that some PN nuclei are H-depleted, thus their energy is supplied by He–burning (see a recent review in Stanghellini 1995). For He–burning stars, the tracks would have similar shapes on the $\log L$–$\log T_{\rm eff}$ diagram to those of H–burning stars, and the mass derivation should not be very different. The only possible caveat concerns stars that burn hydrogen at the AGB, then the H-burning ceases and they switch to helium–burning. Only in this very special case the track on the $\log L$–$\log T_{\rm eff}$ diagram experiences a blue loop, thus the luminosity at a given mass, and for each value of the effective temperature, is not exactly the same than that of H–burning stars. Since the evolutionary timescales of these blue loops are quite short in comparison with the overall post–AGB evolution, we conclude that our mass determination based on the usual H–burning tracks is reliable.

(*iv*) In order to calculate MS masses from the CS masses discussed above, we use the empirical initial mass–final mass relation derived by Weidemann (1987) from observation of field white dwarfs. Given that this method is not model–dependent, we prefer this approach instead of using models of post–AGB evolution for our calculations.

In the following sections we illustrate the post–AGB and progenitor mass derivation of the RBWB sample PNs. In Table 1 we list the usual PN name, the size in arcsec, the statistical and individual distances in kpc, the He II Zanstra temperature, the luminosity, the CS mass, the progenitor mass calculated with the statistical (index [s]), and the individual distance (index [i]). The best mass and distance determinations are in boldface. Table 1 clearly shows

that the PNs of the sample have masses lower than $\sim 2\ M_\odot$, NGC 6720 being a marginal case. In such a range, the proposed extra-mixing mechanism, active prior to the PN ejection, should have effectively destroyed all the ^{3}He.

3.1. IC 289

IC 289 is an irregular multiple shell PN (Chu, Jacoby & Arendt 1987) whose CS magnitudes are known in terms of lower limits only ($B > 15.1$, $V > 15.9$, Shaw & Kaler 1985). By using these lower limits, we produce upper limits to the He II Zanstra temperature and luminosity. The statistical distance is $D(\mathrm{s}) = 1.43$ kpc (CKS), and the individual distance is $D(\mathrm{i}) = 2.71$ kpc (Kaler & Lutz 1985). We obtain $\log T_{\mathrm{eff}} = 4.965 \pm 0.034$, and $\log L/L_\odot = 3.51 \pm 0.16$ by using the statistical distance, and $\log L/L_\odot = 4.06 \pm 0.16$ with the individual distance. The errors associated with the Zanstra analysis depend on the intrinsic observing uncertainties of the individual measurements. By placing the CS of IC 289 on the $\log L$–$\log T_{\mathrm{eff}}$ diagram we obtain $M_{\mathrm{CS}}(\mathrm{s}) < 0.58\ M_\odot$ or $M_{\mathrm{CS}}(\mathrm{i}) < 0.75\ M_\odot$ depending on the distance scale used. We should use the statistical distance as a prime indicator, since the wind distances can be overestimated (Kaler 1991, priv. comm.). The empirical initial mass-final mass relation yields $M_{\mathrm{MS}}(\mathrm{s}) = 1.64\ M_\odot$, if the CS mass is calculated with the statistical distance.

3.2. NGC 3242

The physical parameters of this multiple shell, attached halo PN have been extensively discussed in Stanghellini & Pasquali (1995). We thus will not repeat here the analysis that has been performed to obtain the post–AGB mass (M_{CS}=0.56 $M_\odot$ with $D(\mathrm{s}) = 0.88$ kpc). The MS mass, calculated through the empirical initial mass–final mass relation, is $M_{\mathrm{MS}} = (1.2 \pm 0.2)\ M_\odot$. The individual distances available for this nebula, quoted in A92, show a large spread ($< D(\mathrm{i}) > = 0.9 \pm 1$ kpc), and we do not use them in our calculations. Recently, an expansion distance measured with radio observations (Hajian, Phillips & Terzian 1995) places this PN at 0.42 ± 0.16 kpc. The stellar luminosity at this distance will drop down to $\log L/L_\odot = 2.671$, and the corresponding post-AGB mass would lie out of the permitted range.

3.3. NGC 6543

This H-rich WR nucleus (Mendéz 1991) has well-determined magnitudes (A92). The He II and Hβ fluxes are from A92, while the angular diameter is quoted in CKS. We obtain $\log T_{\mathrm{eff}} = 4.854 \pm 0.015$ and $\log L/L_\odot = 3.547 \pm 0.081$ with CKS statistical distance. The only non-statistical distance available to NGC 6543 is the wind distance by Kaler & Lutz (1985), which is very close to the the statistical distance. Other values of $\log T_{\mathrm{eff}}$ found in the literature are within 10 % of our value (see e.g. Bianchi, Recillas & Grewing 1989, Perinotto 1993, Castor et al. 1981). The position on the HR diagram yields a CS mass of $M_{\mathrm{CS}} = (0.58 \pm 0.01)\ M_\odot$, which, compared to the initial mass–final mass empirical relation (Weidemann 1987) gives $M_{\mathrm{MS}}(\mathrm{s}) = (1.6 \pm 0.2)\ M_\odot$.

3.4. NGC 6720

NGC 6720 also hosts a H-rich nucleus (Mendéz 1991). Its statistical distance is $D(\mathrm{s}) = 0.87$ kpc (CKS), and the measured expansion distance is 0.5 kpc (Pottasch 1980). By using the fluxes and angular dimension of CKS and the magnitudes quoted in A92, we find $\log T_{\mathrm{eff}} = 5.148 \pm 0.026$ and $\log L/L_\odot$=2.858 ± 0.070, which translates into a mass of $M_{\mathrm{CS}} = (0.61 \pm 0.03)\ M_\odot$. If we use the expansion distance we obtain $\log L/L_\odot = 2.375 \pm 0.070$, which pushes the stellar mass up to 0.69 $M_\odot$. This second value is also in agreement with the derivation of $M_{\mathrm{V}} = 7.3$ determined by Pier et al. (1993), although this last result is quite fragile. The statistical distance is in agreement with that found by Napiwotzki & Schönberner (1995), $D = 0.99$ kpc. Very recently, Manchado et al. (1996) have found that this nebula has a second, attached shell. If we were to use this second diameter to calculate the statistical distance *à la* CKS, we would have obtained $D = 0.5$ kpc. In conclusion, it is difficult to decide which is the best guess for the distance. We calculate the mass of the progenitor to be $M_{\mathrm{MS}}(\mathrm{s}) = (2.2 \pm 0.6)\ M_\odot$ and $M_{\mathrm{MS}}(\mathrm{i}) = 3.8\ M_\odot$, respectively, but it is clear that more accurate measurements (e.g. with radio expansion velocity) are needed for this object.

3.5. NGC 7009

Another hydrogen–rich nucleus (O(H), Mendéz 1991). The fact that several PNs of our sample have H–rich nuclei is important in that their mass determination from the H-burning post–AGB tracks are very reliable. Its distance measure is controversial: while the statistical distance places it at 1.2 kpc (CKS), the individual distance values quoted in A92 (except the wind and the model-dependent measurements) average to about half of this value. We calculate $\log T_{\rm eff}$ via Zanstra analysis by using the fluxes and dimensions of CKS, and find $\log T_{\rm eff} = 4.965 \pm 0.017$; by using the statistical distance we obtain $\log L/L_{\odot} = 3.41 \pm 0.10$. The effective temperature is well in agreement with other values found in the literature (Pottasch 1993, Heap 1993, Perinotto 1993). If we were to calculate the luminosity with D(i) $= 0.5$ kpc we would have found $\log L/L_{\odot} = 2.646$. The first $\log L/L_{\odot}$value gives a mass of $M_{\rm CS}$(s) $= (0.57 \pm 0.01)$ $M_{\odot}$, while the other calculated luminosity is too low to allow a mass determination. Other authors find slightly higher values for the mass (e.g. $M_{\rm CS} \simeq 0.64$, Heap 1993). The larger distance is supported also by a very recent work by Maciel (1995), who quotes $D = 1.6$ kpc derived via UV and radio kinematics. For the progenitor mass we obtain $M_{\rm MS}$(s) $= (1.4 \pm 0.2)$ $M_{\odot}$; a progenitor mass cannot be given for $D = 0.5$ kpc.

3.6. NGC 7662

The magnitude determinations for this CS are rather poor (A92). We calculate the effective temperature and luminosity using the fluxes and dimensions of CKS. We find $\log T_{\rm eff} = 5.067 \pm 0.071$ and $\log L/L_{\odot} = 3.44 \pm 0.18$ by using the statistical distance (CKS), and $\log L/L_{\odot} = 3.06 \pm 0.18$ with the averaged individual distance (A92). As a result, $M_{\rm CS}$(s) $= (0.59 \pm 0.02)$ $M_{\odot}$, or $M_{\rm CS}$(i) $= 0.56$ $M_{\odot}$ with similar uncertainties. With our mass determination we find $M_{\rm MS}$(s) $= (1.7 \pm 0.3)$ $M_{\odot}$ and $M_{\rm MS}$(i) $= 1.2$ $M_{\odot}$, respectively. Recently, Hajian & Terzian (1996) find a radio expansion distance of $D = 0.79 \pm 0.75$ kpc, in good agreement with the value used here ($D = 0.75$ kpc) and within the range of the statistical distance given by CKS. In conclusion, we calculate the progenitor mass using $D = 0.75$ kpc.

4. The Abundance of ^{3}He in Planetary Nebulae

In order to derive the ^{3}He abundance we model PNs as homogeneous spheres of fully ionized gas. We compute the abundance of ^{3}He in PNs from the line parameters given by RBWB and from our analysis of the PNs physical parameters.

4.1. The Density of ^{3}He$^+$

The ^{3}He$^+$ column density in PNs can be obtained from observations of the hyperfine structure line of ^{3}He$^+$ at $\nu = 8.6656$ GHz:

$$N(^3{\rm He}^+) = \frac{g_l + g_u}{g_u} \frac{8\pi k \nu^2}{hc^3 A_{ul}} \int T_B(v) {\rm d}v, \qquad (1)$$

where $g_u = 1$, $g_l = 3$, $A_{ul} = 1.95436 \times 10^{-12}$ s^{-1} (Gould 1994), and $T_B(v)$ is the brightness temperature profile of the line. For a gaussian line profile,

$$\int T_B {\rm d}v = \frac{1}{2} \sqrt{\frac{\pi}{\ln 2}} T_B^0 \Delta v, \qquad (2)$$

where T_B^0 is the brightness temperature at the center of the line and Δv is the full width at half power.

The brightness temperature T_B^0 is related to the observed beam-averaged brightness temperature T_L, given by RBWB, by:

$$T_B^0 = T_L \frac{\theta_b^2 + \theta_s^2}{\theta_s^2}, \qquad (3)$$

where θ_b and θ_s are the beam and source angular radii, respectively ($2\theta_b = 82''$).

The number of ^{3}He$^+$ atoms per unit volume $n(^3{\rm He}^+)$ can be obtained dividing the column density $N(^3{\rm He}^+)$ by the average optical path $< \Delta s >$ through the source. Representing a PN as a homogeneous sphere of radius $R = \theta_s D$,

the optical path at a position angle θ is $\Delta s(\theta) = 2\sqrt{R^2 - (\theta D)^2}$, and the optical path averaged on the source results $< \Delta s >= \pi R/2 = \pi\theta_s D/2$.

The final expression for $n(^3\mathrm{He}^+)$ is then

$$n(^3\mathrm{He}^+) = 8\sqrt{\frac{\pi}{\ln 2}}\frac{g_l + g_u}{g_u}\frac{k\nu^2}{hc^3 A_{ul}}\frac{\theta_b^2 + \theta_s^2}{D\theta_s^3}T_L\Delta v. \tag{4}$$

Inserting numerical values, we obtain

$$n(^3\mathrm{He}^+) = 22.7\left(\frac{T_L}{\mathrm{mK}}\right)\left(\frac{\Delta v}{\mathrm{km\ s^{-1}}}\right)\left(\frac{D}{\mathrm{kpc}}\right)^{-1}\left(\frac{\theta_s}{''}\right)^{-3}\left(\frac{\theta_b}{41''}\right)^{2}\left(1 + \frac{\theta_s^2}{\theta_b^2}\right)\ \mathrm{cm}^{-3}. \tag{5}$$

4.2. The Density of H^+

For a ionized gas containing H^+, He^+ and He^{2+}, the density of H^+ is related to the density of electrons via

$$n(\mathrm{H}^+) = \frac{n(\mathrm{e})}{1 + y(1+x)},$$

where

$$y = \frac{n(\mathrm{He}^+) + n(\mathrm{He}^{2+})}{n(\mathrm{H}^+)}, \quad x = \frac{n(\mathrm{He}^{2+})}{n(\mathrm{He}^+) + n(\mathrm{He}^{2+})}.$$

The values of y, x (from CKS) and $n(\mathrm{e})$ are shown in columns 2 to 4 of Table 2. With the exception of IC 289, the electronic densities are derived from forbidden line intensities (Stanghellini & Kaler 1989). The values shown are the averages of the mean values for each density indicator. No forbidden line data being available for IC 289, we have computed its electronic density from the radio flux at 5 GHz with the help of the formula given by Gathier (1987):

$$n(\mathrm{e}) = 4.96 \times 10^3\left(\frac{S_{5\,\mathrm{GHz}}}{\mathrm{mJy}}\right)^{1/2}\left(\frac{T_\mathrm{e}}{10^4\ \mathrm{K}}\right)^{1/4}\left(\frac{D}{\mathrm{kpc}}\right)^{-1}\left(\frac{\theta_s}{''}\right)^{-3/2}\epsilon^{1/2}\left[\frac{1 + y(1+x)}{1 + y(1+3x)}\right]^{1/2}\ \mathrm{cm}^{-3}, \tag{6}$$

where we have taken $S_{5\,\mathrm{GHz}} = 212$ mJy (Higgs 1971), the electron temperature $T_\mathrm{e} = 1.55 \times 10^4$ K from CKS, the average θ_s from Table 1, and a filling factor $\epsilon = 1$. We estimate an uncertainty of 10 % on the resulting values of $n(\mathrm{H}^+)$.

The ^{3}He line parameters from RBWB and our derived abundances are listed in the last four columns of Table 2. Given the distance and the line parameters, the resulting range of abundances reflects mainly the uncertainty in the angular radius of the source (see eq. [5]), which we have allowed to vary between the minimun and maximum inner radius of the nebula as given by Chu et al. (1987). Our results agree with those of RBWB. The only exception is for IC 289, for which RBWB obtain a value of 11.6×10^{-4}, outside our range. We cannot identify the source of the discrepancy since the values of the physical parameters adopted for each PN by RBWB are not given. In agreement with RBWB we conclude that the present analysis confirms the fact that the ejecta of stars with masses below $\sim 2.5\ M_\odot$ have abundances a factor 10–100 larger than those observed in the solar system and in the local ISM.

4.3. Comparison with Stellar Evolutionary Models

Having determined the ^{3}He abundance in the six PNs of known progenitor mass, we can now compare these values with the predictions of stellar evolution models. In Figure 2 we show the derived values of the ^{3}He abundance as function of the stellar mass. Going from the values listed in Table 2 to those plotted here, we have assumed that $^3\mathrm{He/H} \simeq {}^3\mathrm{He}^+/\mathrm{H}^+$ (Balser et al. 1994). The boxes represent the uncertainty associated with the mass and ^{3}He abundance determinations. For IC 289 we have also assumed a lower limit of 0.8 $M_\odot$ for the progenitor mass. For the PNs with upper limits on the abundance, the uncertainty in the progenitor mass is indicated by the size of the horizontal bar. The predictions of several stellar evolution models have been considered. From Figure 2 we see that the most recent calculations agree very well with each other, whereas Iben's results give higher ^{3}He abundance at each mass. The source of this discrepancy lies on Iben's underestimate of the ^{3}He destruction cross section (see Galli et al. 1995). In any case, all PNs with measured abundance are fully consistent with the theoretical predictions.

In Figure 2 we also show the expected ^{3}He abundance in the case of non-standard mixing. The most extensive calculations are those of Boothroyd (1996), while Hogan (1995) only gives a crude estimate of the equilibrium abundance independent of mass. The detailed calculations indicate that the mass dependence of the destruction of ^{3}He is quite strong, and the resulting abundance decreases sharply for masses below $\sim 2.5\ M_\odot$. The comparison with the observed PNs clearly shows that these stars have not suffered any depletion. Even for the most massive progenitor (NGC 6720), for which the difference between the two cases is smaller, the observed abundance is still a factor ~ 2 above the non-standard curve. We thus conclude that the current observations do not support the conjecture of enhanced ^{3}He depletion in all low–mass stars.

5. Chemical Evolution of ^{3}He

As discussed in Section 1, chemical evolution models adopting standard ^{3}He stellar nucleosynthesis overproduce ^{3}He. In particular, all the galactic models in better agreement with the observational constraints predict ^{3}He abundances largely inconsistent with those observed in the solar system and in the ISM (locally and at different galactic radii), unless they adopt alternative nucleosyntheses with strongly reduced ^{3}He contribution from low and intermediate mass stars of the kind described in Section 2 (see Tosi 1996 and references therein). On the other hand, if all stars with $M \leq 2.5\ M_\odot$were to deplete their envelope ^{3}He down to a mass fraction $X_3 \simeq 1 \times 10^{-5}$, no PN would be able to show abundances 100 times larger as those observed by RBWB. By the same argument, the possibility of a nuclear physics solution to the ^{3}He problem proposed by Galli et al. (1994) should be dismissed.

A possible way out of this inconsistency is that some stars experience the extra-mixing and deplete ^{3}He and some others do not and maintain the high yield predicted by standard nucleosynthesis models. In order to verify whether or not this suggestion can reconcile the galactic requirements with the high ^{3}He abundances of RBWB's PNs, we have computed a series of chemical evolution models with standard and alternative nucleosynthesis prescriptions in varying percentages of low and intermediate mass stars.

To this aim, we have recomputed some of the numerical models discussed by DST. All the results described here refer to DST's model 1, a model consistent with all the major observational constraints of the disk (Tosi 1988a,b, Giovagnoli & Tosi 1995). This model assumes an exponentially decreasing SFR (with e-folding time 15 Gyr), explicitly dependent on both the gas and total mass density currently observed at each galactocentric distance, a constant (in time), uniform (in space) infall rate of 0.004 $M_\odot$ kpc^{-2} yr^{-1} and Tinsley's (1980) initial mass function. For consistency with DST findings on the deuterium evolution, the metallicity of the infalling gas is not primordial and assumed to be 1/5 of solar. The sun is assumed to be located at 8 kpc from the galactic center and to have formed 4.5 Gyr ago. The current disk age is assumed to be 13 Gyr (but see DST for the modest effect of assuming instead an age of 10 Gyr). Based on Tosi's (1996) comparison of the best chemical evolution models currently available in the literature, here we adopt $X_{2,p} = 5 \times 10^{-5}$ and $X_{3,p} = 2 \times 10^{-5}$ as the primordial abundances by mass of deuterium and ^{3}He, respectively.

For the cases with standard stellar nucleosynthesis we have adopted DST's yields; for the cases with ^{3}He depletion induced by extra-mixing we have alternatively adopted either Boothroyd's (1996) detailed values as function of stellar mass, or simply taken the equilibrium value ^{3}He/H=1×10^{-5} for $M < 2.5\ M_\odot$ as in Hogan's (1995) suggestion.

Let us define P_d as the percentage of stars with $M \leq 2.5\ M_\odot$ experiencing extra–mixing and therefore depleting ^{3}He; the remaining $1 - P_d$ fraction of stars have standard ^{3}He yields. Figure 3 shows the evolution in the solar ring of the ^{3}He/H ratio resulting from assuming $P_d = 0$ (DST standard model 1-C-Ib), $P_d = 0.7$, 0.8, 0.9 and Boothroyd's (1996) yields. The vertical bars correspond to the 2-σ ranges of values derived from observations of the solar system and the local ISM (Geiss 1993 and Gloeckler & Geiss 1996, respectively). It is apparent that only with $P_d \leq 0.7$ can the models fit the observed ranges. The long-dashed curve in the Figure shows the effect of assuming $P_d = 0.8$ and Hogan's depletion. Since the latter is more drastic than Boothroyd's, the percentage of depleting stars required to obtain the same agreement with the data is smaller, but the results are qualitatively the same.

Figure 4 shows the ^{3}He/H radial distributions resulting at the present epoch from the models shown in Figure 3. Also shown are the abundances derived by RBWB from H II region radio observations (dots with their error bars) and by Gloeckler & Geiss (1996) from Ulysses data on local ISM (vertical bar for the 2-σ range). To get a radial distribution flat and low enough to fit the data, P_d values larger than 0.7 must be invoked, in agreement with the

results obtained for the local evolution.

We thus suggest that to solve the ^{3}He problem in terms of extra mixing in low and intermediate mass stars, the vast majority of them must be affected by this phenomenon. In this framework, the few PNs observed by RBWB and showing large ^{3}He content must have been selected in the, relatively small, sample of stars without deep mixing. Indeed, the selection criteria for the target PNs (Rood 1996, priv. comm.) were aimed at maximizing the likelihood of detecting the ^{3}He line: (*i*) located at least 500 pc above the galactic plane; (*ii*) medium excitation PNs; (*iii*) PNs with low nitrogen and ^{13}C to avoid objects where mixing could have destroyed ^{3}He. The latter criterion suggests that the possibility that 70-80% of low–mass stars deplete ^{3}He and the remaning 30-20% do not is a viable solution to the ^{3}He problem.

6. Conclusions

We have analyzed the sample of PNs with measured ^{3}He abundance in order to determine the mass of the progenitor stars. We found that all PNs have masses below $\sim 2.5\ M_\odot$, and their observed abundances are in agreement with the predictions of standard nucleosynthesis in low–mass stars. Unless the PN sample of RBWB is confirmed to be highly biased in favour of non-depleting stars, these results would pose severe problems to the non-standard destruction mechanisms recently suggested in order to overcome the long-standing problem of ^{3}He overproduction on the Galactic timescale.

By using models of galactic evolution of ^{3}He with standard and non-standard nucleosynthesis prescriptions, we have found that the resulting evolution of ^{3}He can be consistent with the values determined in the pre-solar material and in the local ISM only if more than 70–80 % of the whole population of stars with mass below $\sim 2.5\ M_\odot$ has undergone enhanced ^{3}He depletion. This implies that either the sample of PNs studied here is not representative of the low–mass stellar population, or the solution to the ^{3}He problem lies elsewhere. As for the former possibility, a crucial observational test would be the simultaneous determination of the ^{3}He abundance and the ^{12}C/^{13}C ratio in a large sample of PNs. In fact, in addition to the ^{3}He depletion, extra-mixing during the AGB phase would also decrease the ^{12}C/^{13}C ratio from to the standard value of $\simeq 30$ to $\simeq 5$ (see e.g. Sackmann & Boothroyd 1996). Such small values have been observed in few PNs (Bachiller et al. 1996), although for the only PN (NGC 6720) of known ^{3}He abundance the ^{12}C/^{13}C is consistent with standard predictions. Extending this kind of observations to a statistically significant number of PNs will shed new light on the long standing problem of ^{3}He.

Given the size and the selection criteria mentioned in the previous Section, the RBWB sample of PNs is too small and selective to draw firm conclusions about the generality of the depletion processes taking place in the latest stages of stellar evolution. Observations of the same kind, but on a much larger sample, including also *depleting candidates*, i.e. PNs with high nitrogen and ^{12}C/^{13}C are necessary to finally understand both the late evolutionary phases of low–mass stars and the galactic evolution of an important cosmological baryometer like ^{3}He.

It is a pleasure to thank Dr. A. Boothroyd for providing the extra–mixing yields prior to publication; Dr. C. Charbonnel for her careful reading of the manuscript and valuable comments; Dr. R. T. Rood for useful discussions on the ^{3}He measurements in PNs. D.G. wishes to thank the Institute for Nuclear Theory at the University of Washington for its hospitality and the Department of Energy for partial support during the completion of this work. L.S. acknowledges the warm hospitality of the STScI where part of this work was carried out.

Table 1. Distances, Temperatures, Luminosities and Masses of Central Stars, and Progenitor Masses

PN name	θ [a] ($''$)	D(s) (kpc)	D(i) (kpc)	$\log \frac{T_{\rm eff}}{\rm K}$ [b]	$\log \frac{L({\rm s})}{L_\odot}$	$\log \frac{L({\rm i})}{L_\odot}$	$M_{\rm CS}$(s) ($M_\odot$)	$M_{\rm CS}$(i) ($M_\odot$)	$M_{\rm MS}$(s) ($M_\odot$)	$M_{\rm MS}$(i) ($M_\odot$)
IC 289	18	**1.43**	2.71	$< 4.965 \pm 0.034$	$< 3.51 \pm 0.16$	< 4.060	< 0.58	< 0.75	< **1.6**	< 4.7
NGC 3242	16	**0.88**	0.42	4.963 ± 0.009	3.318 ± 0.030	2.671	0.56 ± 0.01	–[d]	**1.2 ± 0.2**	–[d]
NGC 6543	9.4	**0.98**	0.89	4.854 ± 0.015	3.547 ± 0.081	3.461	0.58 ± 0.01	0.57	**1.6 ± 0.2**	1.4
NGC 6720	34	**0.87**	0.5	5.148 ± 0.026	2.858 ± 0.070	2.375	0.61 ± 0.03	0.69	**2.2 ± 0.6**	3.8
NGC 7009	14	**1.2**	0.5[e]	4.965 ± 0.017	3.41 ± 0.10	2.646	0.57 ± 0.01	–[d]	**1.4 ± 0.2**	–[d]
NGC 7662	7	1.16	**0.75**[e]	5.067 ± 0.071	3.44 ± 0.18	3.060	0.59 ± 0.02	0.56	1.7 ± 0.3	**1.2**

[a] from CKS

[b] He II Zanstra temperatures

[c] same uncertainty as in $\log L$(s)

[d] off permitted range

[e] average values: $\sigma_{\rm NGC7009} = 0.08$; $\sigma_{\rm NGC7662} = 0.32$

Table 2. Abundances in PNs

PN name	$y^{(a)}$	$x^{(a)}$	$n(\mathrm{e})^{(b)}$ (cm^{-3})	$n(\mathrm{H}^+)$ (cm^{-3})	$T_L^{(c)}$ (mK)	$\Delta v^{(c)}$ (kms^{-1})	$n(^3\mathrm{He}^+)$ (cm^{-3})	$^3\mathrm{He}^+/\mathrm{H}^+$ $\times 10^4$
IC 289	0.110	0.448	7.34×10^2	6.33×10^2	2.75	37.73	0.25–0.55	**3.9–8.7**
NGC 3242	0.100	0.187	2.69×10^3	2.40×10^3	4.16	47.24	1.6–5.4	**6.7–22**
NGC 6543	0.111	0.000	1.95×10^3	1.76×10^3	<4.82	56.50	<(5.8–9.1)	<**(33–52)**
NGC 6720	0.113	0.231	4.90×10^2	4.30×10^2	2.85	36.55	0.066-0.13	**1.5–3.0**
NGC 7009	0.112	0.113	4.07×10^3	3.62×10^3	<3.64	43.82	<(2.1–11.3)	<**(5.8–31)**
NGC 7662	0.107	0.287	2.63×10^3	2.31×10^3	<6.98	40.73	<(9.1–26)	<**(39–112)**

(a) from CKS

(b) from Stanghellini & Kaler (1989), except IC 289 (see text)

(c) from RBWB

REFERENCES

Acker, A., Ochsenbein, F., Stenholm, B., Tylenda, R., Marcout, J., & Schohn, C. 1992, Strasbourg–ESO Catalogue of Galactic Planetary Nebulae (Garching: ESO) (A92)

Bachiller, R., Forveille, T., Huggins, P. J., Cox, P., & Omont, A. 1996, in preparation

Balser, D. S., Bania, T. M., Brockway, C. J., Rood, R. T., & Wilson, T. L. 1994, ApJ, 430, 667

Bianchi, L., Recillas, E., & Grewing, M. 1989, in IAU Symposium 155, Planetary Nebulae, ed. S. Torres-Peimbert, p. 307

Boothroyd, A. I. & Sackmann, I.-J. 1995, preprint astro-ph/9512121

Boothroyd, A. I. & Malaney, R. A. 1996, preprint astro-ph/9512133

Boothroyd, A. I. 1996, priv. comm.

Cahn, J. H., Kaler, J. B., & Stanghellini, L. 1992, A&AS, 94, 399 (CKS)

Castor,J. I., Lutz, J. I., & Seaton, M. J. 1981, MNRAS, 194, 547

Charbonnel, C. 1994, A&A, 282, 811

Charbonnel, C. 1995, ApJ, 453, L41

Chu, Y.-H., Jacoby, G. H., & Arendt, R. 1987, ApJSS, 64, 529

Dearborn, D. S. P., Steigman, G., & Tosi, M. 1996, ApJ, 492, (DST)

Denissenkov, P. A. & Weiss, A. 1996, A&A, 308, 773

Fields, B. D. 1996, ApJ, 456, 478

Galli, D., Palla, F., Straniero, O., Ferrini, F. 1994, ApJ, 432, L101

Galli, D., Palla, F., Ferrini, F., Penco, U. 1995, ApJ, 443, 536

Geiss, J. 1993, in Origin and evolution of the elements, eds. N. Prantzos, E. Vangioni-Flam, & M. Cassé (Cambridge Univ. Press), p.89

Gathier, R. 1987, A&AS, 71, 245

Giovagnoli, A. & Tosi, M. 1995, MNRAS, 273, 499

Gloeckler, G. & Geiss, J. 1996, Nat., 381,210

Gould, R. J. 1994, ApJ, 423, 522

Hajian, A. R., Phillips, J. A., & Terzian, Y. 1995, AJ, 109, 2600

Hajian, A. R. & Terzian, Y. 1996, PASP, 108, 258

Heap, S. R. 1993, in IAU Symposium 155, Planetary Nebulae, eds. R. Weinberger & A. Acker (Dordrecht: Kluwer), p.23

Higgs, L. A. 1971, MNRAS, 153, 315

Hogan, C. J. 1995, ApJ, 441, L17

Iben, I. 1967, ApJ, 147, 650

Kaler, J. B. 1983, ApJ, 271, 188

Kaler, J. B. & Lutz, J. H. 1985, PASP, 97, 700

Maciel, W. J. 1995, Ap&SS, 229, 203

Manchado, A., Guerrero, M. A., Stanghellini, L., & Serra-Ricart, M. 1996, The IAC Morphological Catalog of Northern Galactic Planetary Nebulae, IAC (in press)

Mendéz, R. H. 1991, in Evolution of Stars: The Photospheric Abundance Connection, eds. G. Michaud & A. Tutukov (Dordrecht: Reidel), p. 375

Napiwotzki, R. & Schönberner, D. 1995, A&A, 301, 545

Olive, K. A., Rood, R. T., Schramm, D. N., Truran, J., Vangioni-Flam, E. 1995, ApJ, 444, 685

Perinotto, M. 1993, in IAU Symposium 155, Planetary Nebulae, eds. R. Weinberger & A. Acker (Dordrecht: Kluwer), p. 57

Pier, J. R., Harris, H. C., Dahn, C. C., & Monet, D. G. 1993, in IAU Symposium 155, Planetary Nebulae, eds. R. Weinberger & A. Acker (Dordrecht: Kluwer), p. 175

Pottasch, S. R. 1980, A&A, 89, 336

Pottasch, S. R. 1989, in IAU Symposium 155, Planetary Nebulae, ed. S. Torres-Peimbert, p. 481

Prantzos, N. 1996, A&A, 310, 106

Rood, R. T., Steigman, G., & Tinsley, B. M. 1976, ApJ, 207, L57

Rood, R. T., Bania, T. M., & Wilson, T. L. 1992, Nat., 355, 618

Rood, R. T., Bania, T. M., Wilson, T. L., & Balser, D. S. 1995, in The Light Element Abundances, ed. P. Crane (Heidelberg: Springer), p. 201 (RBWB)

Sackmann, I.-J, & Boothroyd, A. I. 1996, preprint astro-ph/9512122

Shaw, R. A. & Kaler, J. B. 1985, ApJ, 295, 537

Stanghellini, L. & Kaler, J. B. 1989, ApJ, 343, 811

Stanghellini, L. & Pasquali, A. 1995, ApJ, 452, 286

Stanghellini, L, & Renzini, A. 1993, in IAU Symposium 155, Planetary Nebulae, eds. R. Weinberger & A. Acker (Dordrecht: Kluwer), p. 473

Stanghellini, L. 1995, proceedings of the Ven Workshop on WR–type PN Nuclei, in press

Steigman, G. & Tosi, M. 1992, ApJ, 401, 150

Terzian, Y. 1993, in IAU Symposium 155, Planetary Nebulae, eds. R. Weinberger & A. Acker (Dordrecht: Kluwer), p. 109

Tinsley, B. M. 1980, Fund. Cosmic Phys., 5, 287

Tosi, M. 1988a, A&A, 197, 33

Tosi, M. 1988b, A&A, 197, 47

Tosi, M. 1996, in From Stars to Galaxies, eds. C. Leitherer, U. Fritze-von Alvensleben, & J. Hucra, ASP Conf. Ser. 98, in press

Truran , J. W. & Cameron, A. G. W. 1971, ApJSS, 14, 179

Vangioni-Flam, E., Olive, K. A., & Prantzos, N. 1994, ApJ, 148, 3

Wasserburg, G. J., Boothroyd, A. I., & Sackmann I.-J. 1995, ApJ, 427, 618

Weidemann, V. 1987, A&A, 188, 74

Weiss, A., Wagenhuber, J., & Denissenkov, P. A. 1996, preprint astro-ph/9512120

Yang, J., Turner, M. S., Steigman, G., Schramm, D. N., & Olive, K. A. 1984, ApJ, 281, 493

This preprint was prepared with the AAS LaTeX macros v4.0.

Fig. 1.— Location of the six PNs of the RBWB sample in the H-R diagram. Solid lines are evolutionary tracks from Stanghellini & Renzini (1993) for central stars with masses 0.55, 0.57, 0.58, 0.59, and 0.60 $M_\odot$(bottom to top).

Fig. 2.— ^{3}He abundance (by number with respect to H) versus MS mass for the six PNs of the RBWB sample with the associated range of derived values. The curves show the results of the ^{3}He abundance in the stellar envelope at the end of the RGB phase as computed by: Iben (1967) for $Z = 0.02$ (*solid line*); Rood et al. (1976) for $Z = 0.02$ (*short dashed line*); Boothroyd (1996) for $Z = 0.02$ and $X_{3,\rm MS} = 8.4 \times 10^{-5}$ (*long dashed line*); Weiss et al. (1996) for $Z = 0.02$ and $X_{3,\rm MS} = 6.02 \times 10^{-5}$ (*dot dashed line*); DST for $Z = 0.02$ and $X_{3,\rm MS} = 1.0 \times 10^{-4}$ (*dotted line*). The results of stellar nucleosynthesis ith deep mixing during the RGB phase computed by Boothroyd (1996) are shown as *dot-dashed* lines, and the equilibrium value ^{3}He/H $= 10^{-5}$ for $M < 2.5\ M_\odot$ as a *short dash - long dash* line.

Fig. 3.— Time evolution of ^{3}He/H in the solar neighborhood. The vertical bars (2-σ errors) show the abundance of ^{3}He measured in the solar system (Geiss 1993) and in the local ISM (Geiss & Gloeckler 1996). The curves show the predictions of chemical evolution models assuming different percentages P_d of stars depleting ^{3}He (see text): *solid line* P_d=0 with DST standard stellar yields (*solid line*); P_d=0.7, 0.8 and 0.9 with Boothroyd's (1996) yields (*dash-dotted, dotted* and *dashed lines*); $P_d = 0.8$ with Hogan's (1995) depleted yields (*long-dashed line*).

Fig. 4.— Radial distribution of ^{3}He/H as derived from H II region observations (dots and error bars from RBWB) and from chemical evolution models for the present epoch. The vertical bar gives (at 2-σ) the value measured in the local ISM (Geiss & Gloeckler 1996). The line symbols are as in Figure 3.

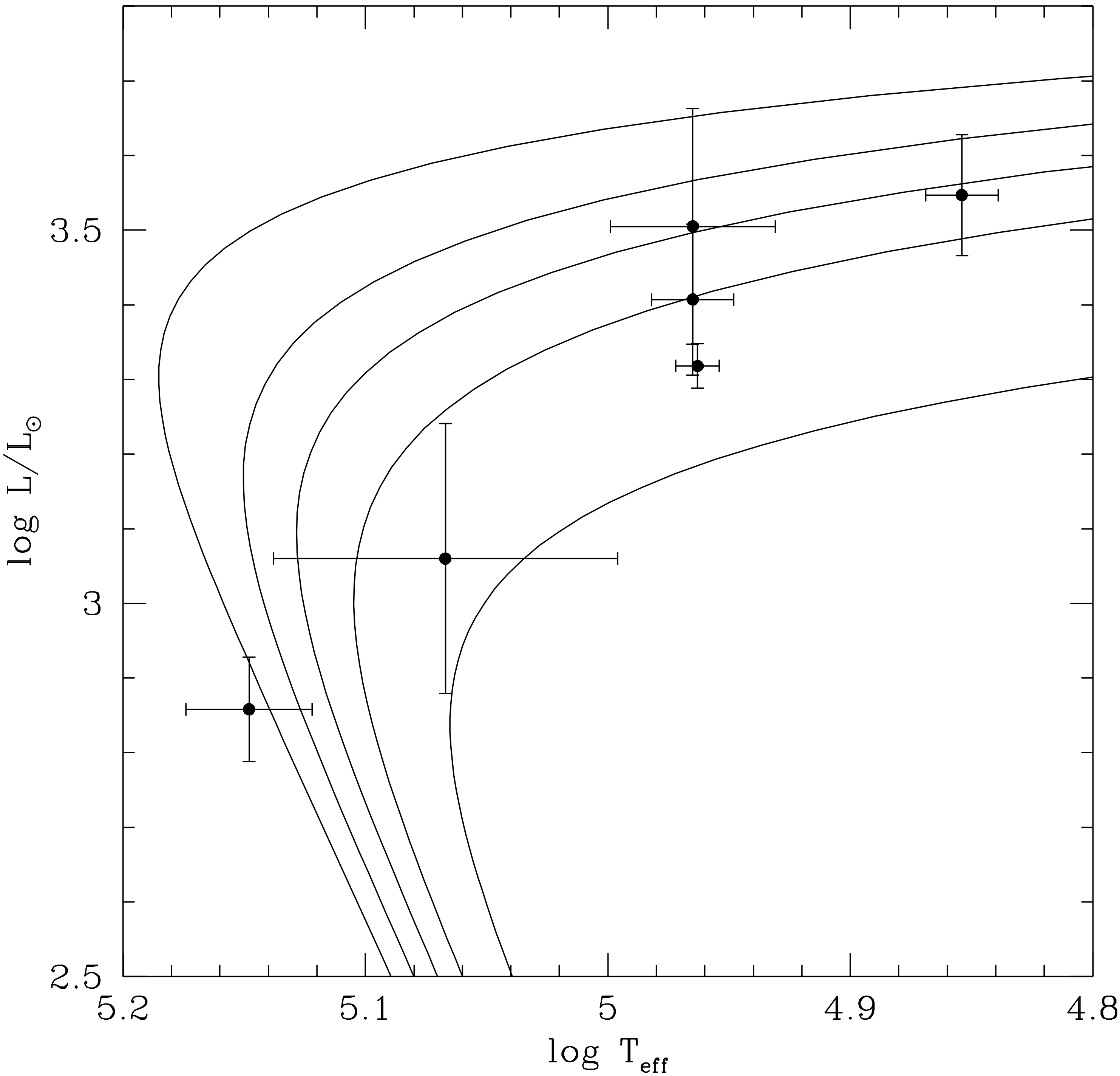

3.5
3
2.5
log L/L$_\odot$
5.2
5.1
5
4.9
4.8
log T$_{eff}$

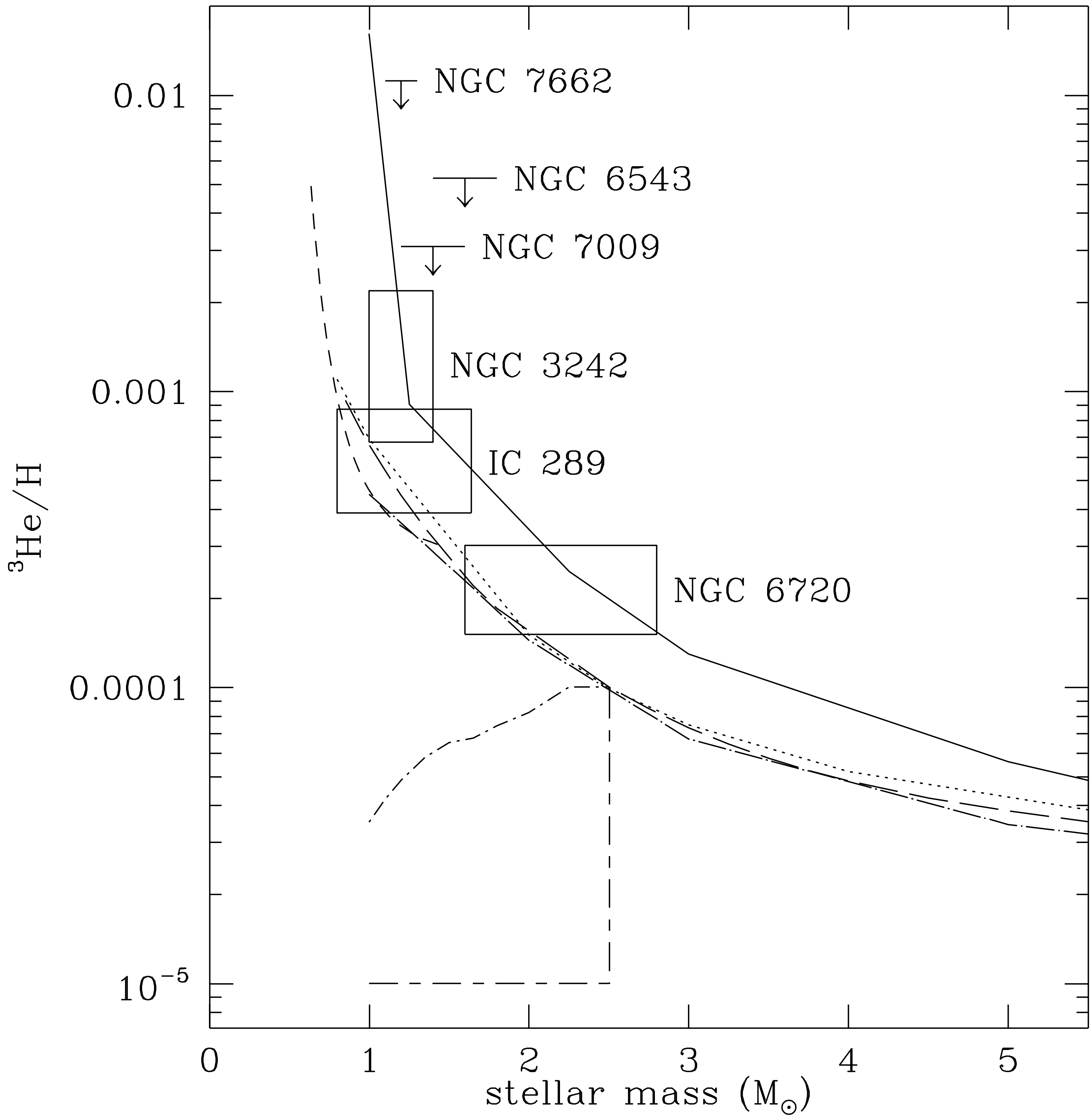

NGC 7662
NGC 6543
NGC 7009
NGC 3242
IC 289
NGC 6720
0.01
0.001
0.0001
10^{-5}
^{3}He/H
0
1
2
3
4
5
stellar mass ($M_\odot$)

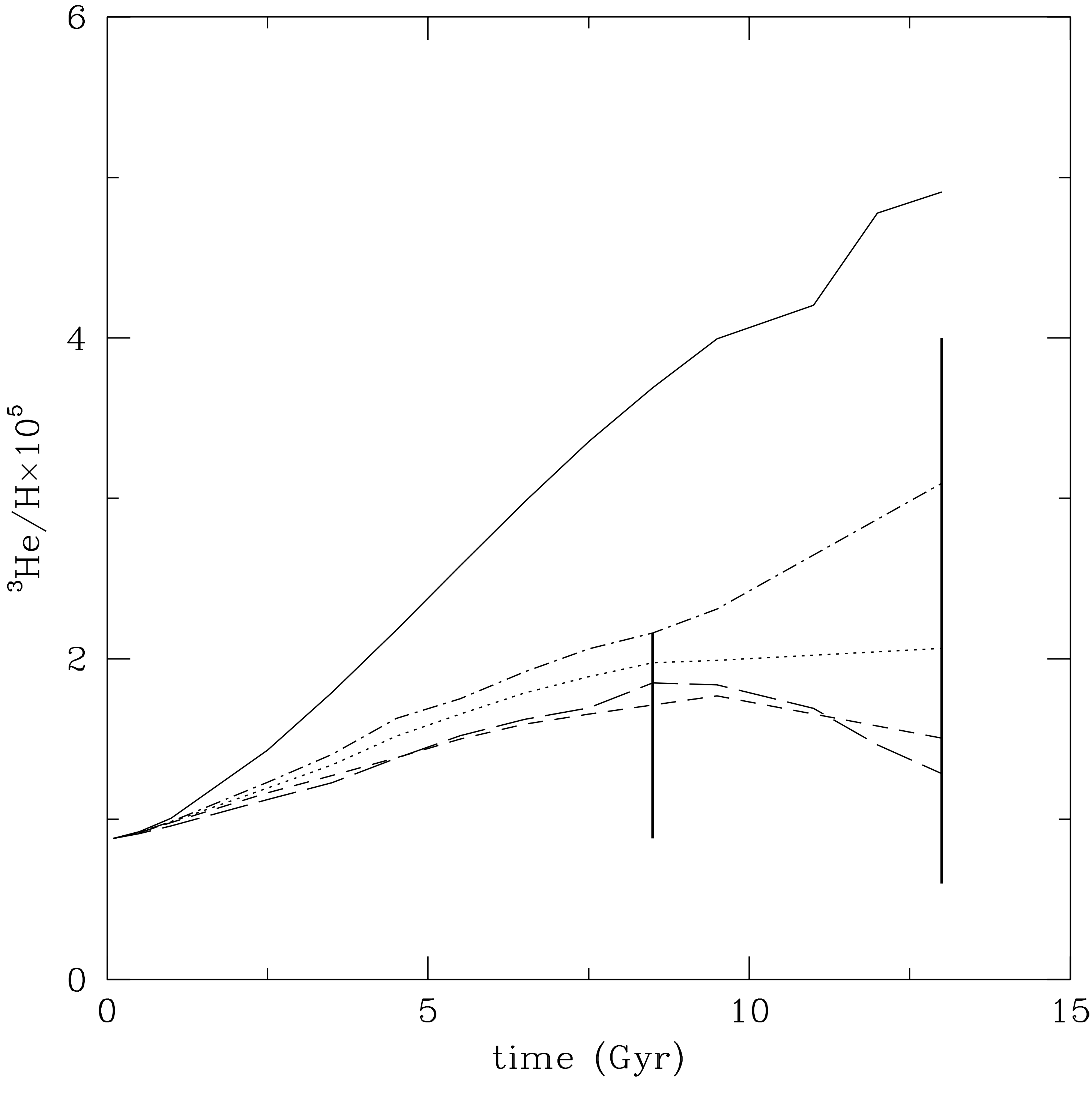

6
4
2
0
0
5
10
15
^{3}He/H×10^5
time (Gyr)

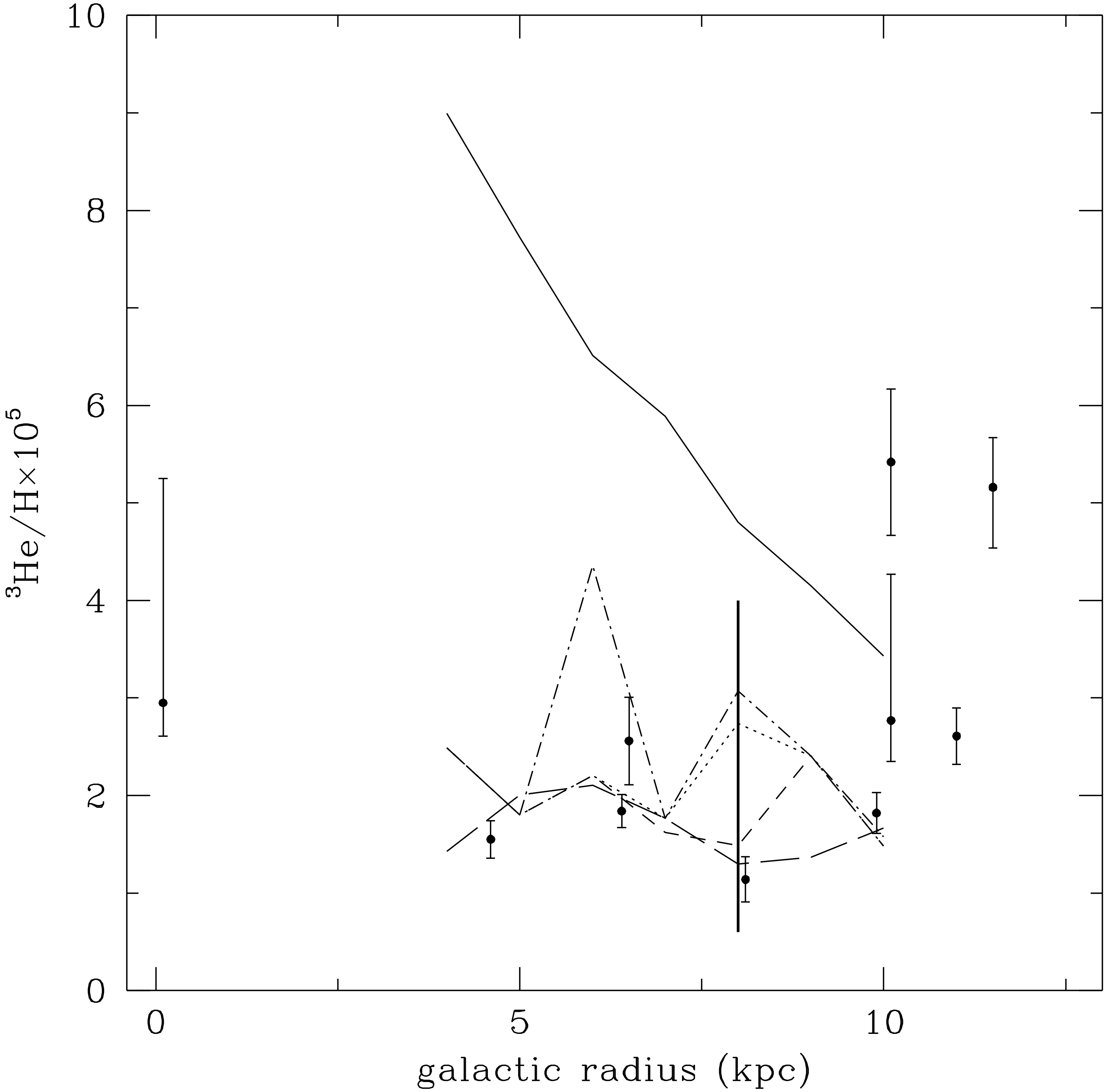

10
8
6
4
2
0
0
5
10
^{3}He/H×10^5
galactic radius (kpc)